Performance Analysis of Multi-hop Wireless Networks under Different Hopping Strategies with Spatial Diversity

Hu Han [1,2], Zhu Hongbo[1,2] and Zhu Qi [1,2]

[1]Jiangsu Key Lab of Wireless Communications

[2] Key Lab on Wideband Wireless Communications and Sensor Network Technology of Ministry of Education, Nanjing University of Posts and Telecommunications, Jiangsu Nanjing 210003, China

[e-mail: huhan68@163.com; zhuhb@njupt.edu.cn; zhuqi@njupt.edu.cn]

*Corresponding author: Hu Han

Received May 15, 2012; revised July 15, 2012; revised August 30, 2012; accepted September 30, 2012; published October 29, 2012

Abstract

This paper derives two main end-to-end performance metrics, namely the spatial capacity density and the average end-to-end delay of the multi-hop wireless ad hoc networks with multi-antenna communications. Based on the closed-form expressions of these performance metrics, three hopping strategies, i.e., the closest neighbor, the furthest neighbor and the randomly selected neighbor hopping strategies have been investigated. This formulation provides insights into the relations among node density, diversity gains, number of hops and some other network design parameters which jointly determine network performances, and a method of choosing the best hopping strategy which can be formulated from a network design perspective.

Keywords: Performance metrics, network design, stochastic geometry, hopping strategy, statistical mechanics, multi-antenna

This work is supported by the National Natural Science Foundation of China (61171094), the Important National Science and Technology Specific Project(2011ZX03001-006-02,2011ZX03005-004-03),the Graduate Student Innovation Plan of Jiangsu Province(CXZZ11_0387) and the Key Project of Jiangsu Provincial National Science Foundation(BK2011027))

http://dx.doi.org/10.3837/tiis.2012.10.006

1. Introduction

One of the best known metrics for studying end-to-end network capacity is transport capacity [1], which is proposed to quantify the number of bits-meters per second a wireless network can sustain when its density grows to infinite. The framework of transport capacity pioneered many notable studies on the limiting scaling behavior of ad hoc networks under various models of node interaction and fading conditions, including [2][3], and the complications of such studies are stated therein. Nevertheless, their analyses focus on a deterministic SINR model and employ a deterministic channel access scheme, which is not a good way to evaluate the performance of specific communicaiton strategies and how their network parameters imposed by a specific transmission strategy affect the throughput capacity.

In order to accurately model the behavior of a distributed ad hoc network at the physical and MAC layer, Weber et al. [4] incorporated a stochastic SINR-based model and defined the transmission capacity as the product of the maximum density of successful transmission and the corresponding data rate, under a constraint on the outage probability. The key to this approach is to assume the locations of nodes over the plane are random, particularly modeled as a homogenous Poisson point process (HPPP) using the tools from stochastic geometry [5][6]. And it was proven in [7] that transport capacity and transmission capacity are consistent in the scaling sense yet complementary to each other. The former gives order optimal throughput, optimized over all MAC and routing techniques, while the latter allows for tractable analysis with different physical layer transmission techniques, such as power control [8], interference cancellation[9], and channel inversion[10].

Most of the aforementioned work on computing the transmission capacity of ad hoc networks has been limited to single-hop communications as it considers a snapshot of the typical network only. Recent research has begun to investigate new metrics to describe capacity of the multi-hop networks. In [11], Andrews et al. extended the transmission capacity framework and proposed random-access transport capacity (RTC) to obtain the optimal number of hops that maximize RTC, under the assumption that hop lengths are all equidistant on a straight line and delay-energy constraint is relaxed. In [12], Vaze studied the tradeoff between the throughput, delay and reliability, using the RTC in the scenario where the multi-hop links are constrained by a maximum allowed delay. In contrast to [11], Vaze's study considered the spatial and temporal correlation of the interference but did not assume independence of success/failure of packets across time slots. In [13], Nardelli et al. suggested using aggregate multi-hop information efficiency (AMIE) to quantify the spatial efficiency of information bit transmission. This metric was also applied to determine whether a large number of short single-hop links or a small number of long single-hops is preferable in a multi-hop wireless network in [14]. However, most of the aforementioned work about multi-hop communications is under the assumption that each S-D pair only transmits a single packet at a time along the entire multi-hop path. In this circumstance, only one single link of a typical route at a time is considered, relays are always located along the source-destination axis and the hop lengths all equidistant. This is an ideal assumption not applicable to real systems. For this reason, [15] exploited the analogy between the transport of packets in multi-hop wireless line networks and flow of particles in TASEP model [16].

In this paper, we seek to explore a new approach to describe the network capacity and related metrics of multi-hop multi-antenna ad hoc networks, and identify the best hopping

strategy in the multi-hop multi-antenna networks from three hopping strategies, i.e., the closest neighbor, furthest neighbor and randomly selected neighbor strategies. We consider an ad hoc network where node locations are assumed to be a realization of homogenous Poisson process, which provides a tractable way to evaluate the per-hop success probability across different hops in multi-antenna systems. The totally asymmetric simple exclusion process (TASEP), a similar approach as demonstrated in [15], is then employed to characterize the end-to-end performance metrics of a typical source-destination route in the multi-hop multi-antenna network. Based on the network model and traffic model, some insights into the best hopping strategy which are conducive to network designing are provided, with the closed-form expressions of two main end-to-end performance metrics, namely the spatial capacity density and average end-to-end delay. Our results show that the best hopping strategy is closely related to the level of received signal and interference which can be well controlled by the design parameters such as node density, the number of antennas, et al.

Our main contributions are the following: (1) Closed-form expressions of two main end-to-end performance metrics in multi-hop multi-antenna wireless networks, the spatial capacity density and the average end-to-end delay, are derived using concepts and tools from stochastic geometry and TASEP. This contributes to understanding of the relations among node density, diversity gains, number of relays and related network parameters. (2) The fomulation proposed allows us to identify the best hopping strategy (from the closest neighbor, the furthest neighbor and the randomly selected neighbor hopping) under different network operating conditions, which is interested when designing real ad hoc networks.

The remainder of the paper is organized as follows. Section 2 presents the system models, hopping strategies and the definitions of the performance metrics used in this study. Key findings of our research such as the closed-form expressions of per-hop success probability, spatial capacity density and average end-to-end delay are listed in Section 3. Implications and interpretations of these results are provided in Section 4 and Section 5 arrives at a conclusion.

2. System Model

2.1 Models And Assumptions

We consider an ad hoc network comprised of infinite number of nodes randomly located on a planer network following a homogeneous Poisson point process (PPP), with density λ_0 per unit area. Assuming each node has an infinite number of packets to transmit and access the common medium according to slotted ALOHA protocol with a predefined transmission probability q. The sets of nodes could be divided into two independent PPP with a countable infinite population of source nodes of density $\lambda_s = q\lambda_0$ and the other nodes (potential relays and destination) of density $\lambda_r = (1-q)\lambda_0$, according to the property of independent thinning of PPP[5]. Also assume that each source node initiates a flow of packets to a certain destination node at a random direction and a random finite distance lasting over an infinite duration of time.

Slivnyak's theorem[5] from stochastic geometry states that an entire homogeneous network can be characterized by a typical single transmission. Conditioning on a typical pair which we refer to as TX_0 and RX_0, from the perspective of RX_0, the spatial point process of the set of interferes (which is the entire transmit process with the exception of TX_0) is still homogenous

with the same statistics. So in the following, it is feasible to analyze a "typical" flow in the system as the distribution of nodes is homogeneous. All the results are obtained upon averaging over all possible realizations of the underlying point processes.

In this paper, multi-antenna communications are considered in the multi-hop wireless network. For simplified analysis, we assume that each node uses a single transmit antenna and L received antennas or the SIMO(Single Input Multiple Output) transmissions. A transmitted signal undergoes both large-scale fading with a path-loss exponent α greater than 2 and small-scale Rayleigh fading where fading exponent is exponentially distributed with mean of unit. For a interference-limited system, the noise is negligible compared to interference[7], and thus the L-dimensional received signal y_0 at a typical receiver RX_0 is given by

$$y_0 = d_0^{-\alpha/2} h_0 u_0 + \sum_{i \in \Pi(\lambda_I)} |X_i|^{-\alpha/2} h_i u_i \tag{1}$$

Where $|X_i|$ is the distance from $\mathrm{TX_i}$ to RX_0, h_i is the vector channel from $\mathrm{TX_i}$ to RX_0, and u_i is the power-P symbol transmitted by $\mathrm{TX_i}$. Considering in a rich scattering environment, each of the vector channel h_i has i.i.d unit-various complex Gaussian components, i.e., $[h_i]_k \sim CN(0,1), 1 \le k \le L$ independent across transmitters.

At the physical layer, a data packet is said to be successfully captured by a receiver node if the signal-to-interference-plus-noise ratio (SINR) perceived by this node exceeds a prefix threshold β. In the interference-limited system, we can use signal-interference-ratio (SIR) to replace SINR.

For Maximal Ratio Combiner (MRC), the data estimate is formed via $\hat{y}_0 = h_0^{\dagger} y_0$, where $(\cdot)^{\dagger}$ denotes conjugate transpose, from which the resulting SIR can be written as:

$$\begin{aligned} SIR &= \frac{P \left| h_0^{\dagger} h_0 \right|^2 R^{-\alpha}}{\sum_{i \in \Pi(\lambda_I)} P \left| h_0^{\dagger} h_i \right|^2 |X_i|^{-\alpha}} \\ &= \frac{\|h_0\|^2 R^{-\alpha}}{\sum_{i \in \Pi(\lambda_I)} \left| \frac{h_0^{\dagger} h_i}{\|h_0\|} \right|^2 |X_i|^{-\alpha}} \end{aligned} \tag{2}$$

Where $\|\cdot\|$ is the modular arithmetic and λ_I is the density of the interfering nodes whose value will be given in the later. Note that in our multi-hop multi-antenna model, all interferes are not only the sourcing nodes, but also the nodes selected as relays according to some pre-determined hopping strategies.

2.2 Hopping Strategies

A typical multi-hop transmission scenario is considered, where a data source sends information to its final destination through N+1 hops, which means each flow occurs across N relay nodes. To ensure a next hop RX exists at a proper position, a selection region of neighborhood sets based on hop routing protocol is given similar to that proposed in [17]. The selection region contains a set of potential receivers located in the circle centered at TX, with

radius of the maximum transmission distance r_m and the angle $\psi \in (0, \pi)$. Note that the angle defining the neighborhood of a TX must be smaller than π to ensure that the packets are forwarded towards their destinations. At each hop, the TX selects a RX as the relay in its selection region based on its distance to their neighborhood. In this work, three hopping strategies are considered at each hop, the closest neighbor, the furthest neighbor and the randomly selected neighbor hopping strategies[18].

Fig.1 illustrates the selection region of a TX. TX is placed in the circle center. The maximum transmission distance is denoted by r_m. Assuming that the angle with which each packet traversed at each hop to the destination is denoted by the random variable ϕ and is uniformly distributed in $(-\psi/2, \psi/2)$.The blue-colored triangles represent potential RXs which are within the selection region of this TX. Clearly RX_C and RX_F represent the closest and furthest neighbors, respectively.

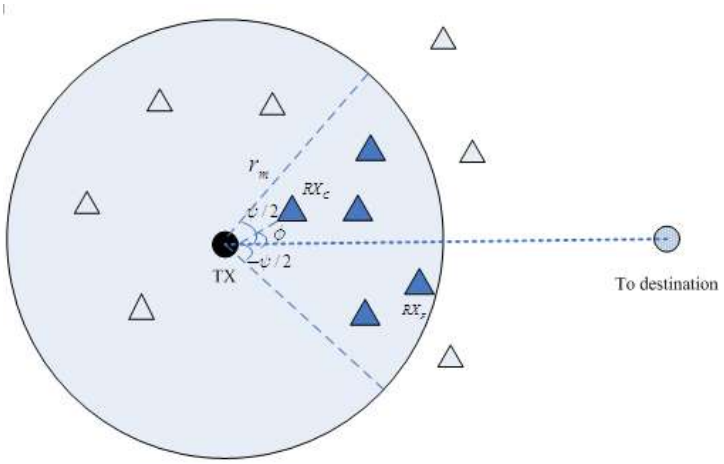

Fig. 1. Illustration of a selection region

For the closest or furthest neighbor hopping strategies, when there are more than one RXs with the same closest or furthest distances appear in the selection region of a TX, this TX will randomly choose a RX as its next hop relay. And if more than one TXs select the same node as the next hop relay, one of those TXs will be selected randomly to pair up with that RX node, while the others will all be set as inactive during that given time-slot.

2.3 Transmission Policy And Performance Metrics

In this paper, the same transmission policy is employed for the multi-hop multi-antenna wireless network as described in [15]. In order to exploit the analogy between the transport of packets in multi-hop wireless line networks and flow of particles in the TASEP model, it is assumed that each relay node has buffer size of unity. In other words, if their buffer already contains a packet, transmissions will not be accepted by that relay node. Meanwhile, retransmission scheme is also assumed. Packets are retransmitted until they are successfully received which is necessary to keep the network at a total reliability. More superiorities about this simplified transmission can be found in [15].

Fig.2 illustrates the workflow of a packet delivered between the source and destination node when adopting closest neighbor hopping strategy. Each destination node is assumed to

be located 3 closest-neighbor hops away from its corresponding source node. The mechanics can be described as follows:

1) According to the closest neighbor hopping strategy, the source node chooses the closest neighbor in its selection region as the 1st relay node of the typical routing. If the next hop relay is unavailable, the source node will be set as inactive during that given time-slot. And in the next time-slot, the closest neighbor selection process will be carried out again. Else, jump to step 2.
2) If the per-hop transmission between the source node and the 1st relay node is successful, then go to step 3, otherwise, jump to step 4.
3) The 1st relay node selects its own closest neighbor as the 2nd relay node of the typical routing. If the next hop relay is not available, the 1st relay node will be set as inactive during that given time-slot. And in the next time-slot, the closest neighbor selection process will be carried out again. Else, jump to step 5.
4) The packet from the source node to the 1st relay node is retransmitted until it is successfully received by the 1st relay node.
5) If the per-hop transmission between the 1st and 2nd relay is successful, then move to step 6, else go straight to step 7.
6) If the per-hop transmission between the 2nd relay node and the destination node is successful, then the work flow is carried out, else jump to step 8.
7) The packet from the 1st and 2nd relay node is retransmitted until it is successfully received by the 2nd relay node.
8) The packet from the 2nd relay node and destination node is retransmitted until it is successfully received by the destination node, then the work flow is carried out.
9)

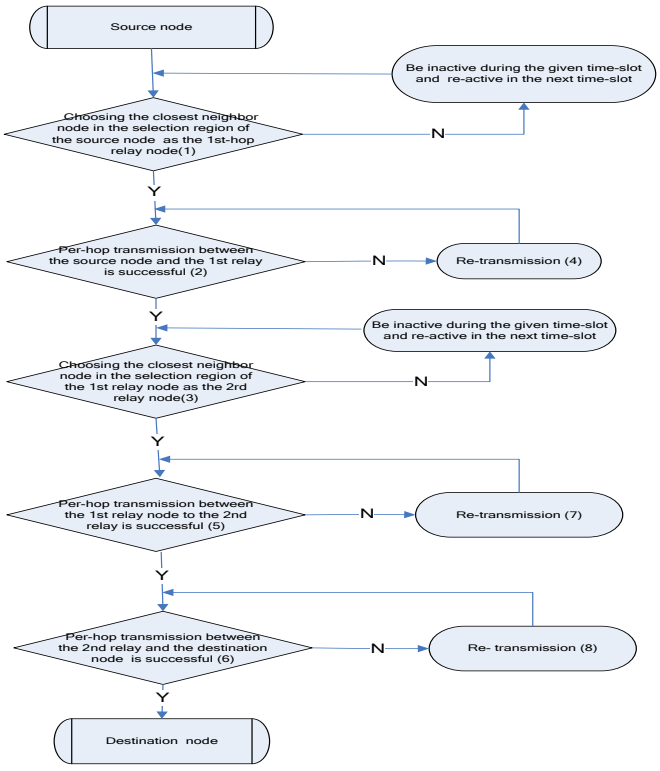

Fig. 2. Workflow of a packet delivered between the source and destination node

As illustrated in [19], the performance of the networks is mainly characterized based on the following two end-to-end metrics, spatial capacity density and the average end-to-end delay. They and some other basic metrics are defined as follows:

- The per-flow **throughput** T, is defined as the average number of packets successfully delivered to the destination in unit time along a typical flow in the network.
- The **expected total progress** D, is defined as the effective distances traveled along the axis to the destination which can be given by $D=(N+1)E[R\cos(\Phi)]$. R is the single-hop transmission distance from the origin TX to its associated RX, and Φ is the angle with which each packet traversed at each hop to the destination (see **Fig. 1.**) .
- The **spatial capacity density** C_{tran}, is defined as the average number of bit-meters successfully delivered per unit time per unit area. We take it as a product of the throughput of a typical flow T, the expected total progress D and the density of the source nodes λ_s which can be given by $C_{tran}=\lambda_s TD$.
- The **average end-to-end delay** D_{e2e}, is a measure of the average number of time-slots it takes for the packet at the head of the source buffer across N relays to be successfully delivered to the destination.

3. Main results

In this Section, we first derive expressions for per-hop success probability with different hopping strategies using stochastic geometry, and then combine with TASEP model to derive the performance metric of the spatial density of transport and the average end-to-end delay.

3.1 Per-Hop Success Probability Analysis With Different Hopping Strategies

Theorem 1: For a single-input multiple-output, or SIMO communication, performing maximal ratio combing with L antennas, the per-hop success probability under Rayleigh fading is given by

$$p_{s|R}(r)\approx 1-\lambda_I \beta^{\frac{2}{\alpha}} r^2 \frac{C_\alpha}{K_\alpha} \tag{3}$$

where $C_\alpha=\frac{2\pi}{\alpha}\Gamma(\frac{2}{\alpha})\Gamma(1-\frac{2}{\alpha})$, $K_\alpha=\left[1+\sum_{k=1}^{L-1}\frac{1}{k!}\prod_{l=0}^{k-1}(l-\frac{2}{\alpha})\right]^{-1}$ and λ_I is the density of the interfering nodes whose value will be given later.

Proof: Recalling that the received SIR depends on the locations of the interfering nodes and the vector channels, both of which are random. The per-hop success probability with respect to a pre-defined SIR threshold is:

$$p_{s|R}=\mathrm{P}(SIR\geq\beta) \tag{4}$$

We denote the signal and interference coefficients as

$$\begin{aligned} S_0&=\|h_0\|^2 \\ S_i&=\left|\frac{h_0^\dagger h_i}{\|h_0\|}\right|^2 \quad i=1,2... \end{aligned} \tag{5}$$

Then (2) could be rewritten as

$$SIR = \frac{S_0 R^{-\alpha}}{\sum_{i \in \Pi(\lambda_I)} S_i |X_i|^{-\alpha}} \tag{6}$$

And the aggregate interference is a Poisson shot noise process, which can be denoted as

$$I = \sum_{i \in \Pi(\lambda_I)} S_i |X_i|^{-\alpha} \tag{7}$$

As shown in [20], for MRC, the coefficient S_0 is χ^2_{2L} with 2L degrees of freedom. The interference terms $S_i (i = 1, 2...)$ are i.i.d. unit-mean exponential (i.e., χ^2_2 with 2 degrees of freedom).

Here we use the approach proposed in [21].The CCDF of S_0 is $F^c_{S_0}(x) = e^{-x} \sum_{k=0}^{L-1} \frac{x^k}{k!}$, then according to [21], the probability of successful transmission for a typical receiver is:

$$\mathrm{P}(SIR \geq \beta) = \sum_{k=0}^{L-1} \frac{(-\xi)^k}{k!} \frac{d^k}{d\xi^k} L_I(\xi) \Big|_{\xi = \beta R^\alpha} \tag{8}$$

where $L_I(\xi)$ is the Laplace transform for a general Poisson shot noise process in a plane. In the light of [22], it can be given by

$$L_I(\xi) = \exp\left\{ \lambda_I \int_{R^2} 1 - E\left[e^{-\xi S |X_i|^{-\alpha}} \right] dx \right\} \tag{9}$$

As S_i in (10) is exponential with mean of unit, the moment generating function of each mark is altered to be

$$E\left[e^{-\xi S |X_i|^{-\alpha}} \right] = \frac{1}{1 + \xi S |X_i|^{-\alpha}} \tag{10}$$

Given (10), $L_I(x)$ can be transformed into

$$\begin{aligned} L_I(\xi) &= \exp\left\{ -\lambda_I \int_{R^2} \left(1 - \frac{1}{1 + \xi |X|^{-\alpha}}\right) dx \right\} \\ &= \exp\left\{ -2\pi\lambda_I \int_0^\infty \frac{1}{1 + |X|^{-\alpha} / \xi} dx \right\} \\ &= \exp(-\lambda_I C_\alpha \xi^{\frac{2}{\alpha}}) \end{aligned} \tag{11}$$

$$\text{where } C_\alpha = \frac{2\pi}{\alpha} \Gamma\left(\frac{2}{\alpha}\right) \Gamma\left(1 - \frac{2}{\alpha}\right) \tag{12}$$

Applying in [21 Theorem 1], for small transmission density, the outage probability with an asymptotic expression is given by

$$\begin{aligned} \mathrm{P}(SIR < \beta) &= \lambda_I \xi^{\frac{2}{\alpha}} C_\alpha \sum_{k=0}^{L-1} \frac{1}{k!} \prod_{l=0}^{k-1} \left(l - \frac{2}{\alpha}\right) + \Theta(\kappa^2) \Big|_{\xi = \beta r^\alpha} \\ &\approx \lambda_I \xi^{\frac{2}{\alpha}} \frac{C_\alpha}{K_\alpha} \Big|_{\xi = \beta r^\alpha} \\ &\approx \lambda_I \beta^{\frac{2}{\alpha}} r^2 \frac{C_\alpha}{K_\alpha} \end{aligned} \tag{13}$$

where $K_\alpha = \left[1+\sum_{k=1}^{L-1}\frac{1}{k!}\prod_{l=0}^{k-1}(l-\frac{2}{\alpha})\right]^{-1}$ and $\Theta(\kappa^2)$ is a small error term which results from the Taylor expansion.

Theorem 2: For the closest neighbor, furthest neighbor and randomly selected neighbor hopping strategies, the per-hop success probabilities are given by

$$p_{s,c} \approx 1-\lambda_I \beta^{\frac{2}{\alpha}} \frac{C_\alpha}{K_\alpha}\left(\frac{r_m^2+\frac{2}{\psi\lambda_r}(1-\exp(\frac{\psi}{2}\lambda_r r_m^2))}{1-\exp(\frac{\psi}{2}\lambda_r r_m^2)}\right) \tag{14}$$

$$p_{s,f} \approx 1-\lambda_I \beta^{\frac{2}{\alpha}} \frac{C_\alpha}{K_\alpha}\left(\frac{r_m^2-\frac{2}{\psi\lambda_r}(1-\exp(-\frac{\psi}{2}\lambda_r r_m^2))}{1-\exp(-\frac{\psi}{2}\lambda_r r_m^2)}\right) \tag{15}$$

$$p_{s,r} \approx 1-\frac{\lambda_I \beta^{\frac{2}{\alpha}} C_\alpha r_m^2}{2K_\alpha} \tag{16}$$

Proof: The PDF of the single-hop transmission distance R for the closest neighbor hopping strategy is given by [23].

$$f_R^c(r) = \frac{\psi r\lambda_r \exp(-\frac{\psi}{2}\lambda_r r^2)}{1-\exp(-\frac{\psi}{2}\lambda_r r_m^{\ 2})} \quad 0<r<r_m \tag{17}$$

Combining (3) and (17), the per-hop success probability of a packet transmission across the closest neighbor can be expressed as

$$\begin{aligned} p_{s,c} &\approx 1-\int_0^{r_m}\frac{\psi r\lambda_r \exp(-\frac{\psi}{2}\lambda_r r^2)}{1-\exp(-\frac{\psi}{2}\lambda_r r_m^{\ 2})}\lambda_I \beta^{\frac{2}{\alpha}} r^2 \frac{C_\alpha}{K_\alpha}dr \\ &= 1-\frac{\psi\lambda_r\lambda_I\beta^{\frac{2}{\alpha}}\frac{C_\alpha}{K_\alpha}}{1-\exp(-\frac{\psi}{2}\lambda_r r_m^{\ 2})}\int_0^{r_m} r^3\exp(-\frac{\psi}{2}\lambda_r r^2)dr \\ &= 1-\lambda_I\beta^{\frac{2}{\alpha}}\frac{C_\alpha}{K_\alpha}\left(\frac{r_m^2+\frac{2}{\psi\lambda_r}(1-\exp(\frac{\psi}{2}\lambda_r r_m^{\ 2}))}{1-\exp(\frac{\psi}{2}\lambda_r r_m^{\ 2})}\right) \end{aligned} \tag{18}$$

The PDF of the single-hop transmission distance R for the furthest neighbor and randomly selected neighbor hopping strategy is given by[23]

$$f_R^f(r) = \frac{\psi r\lambda_r \exp(-\frac{\psi}{2}\lambda_r(r_m^{\ 2}-r^2))}{1-\exp(-\frac{\psi}{2}\lambda_r r_m^{\ 2})} \quad 0<r<r_m \tag{19}$$

Putting together (3) and (19), the per-hop success probability of a packet transmission across the furthest neighbor can be written as

$$p_{s,f} \approx 1-\int_0^{r_m} \frac{\psi r \lambda_r \exp(-\frac{\psi}{2}\lambda_r(r_m{}^2 - r^2))}{1-\exp(-\frac{\psi}{2}\lambda_r r_m{}^2)} \lambda_I \beta^{\frac{2}{\alpha}} r^2 \frac{C_\alpha}{K_\alpha} dr$$

$$= 1-\frac{\psi\lambda_r\lambda_I\beta^{\frac{2}{\alpha}}\frac{C_\alpha}{K_\alpha}}{1-e^{(-\frac{\psi}{2}\lambda_r r_m{}^2)}} \int_0^{r_m} r^3 \exp(-\frac{\psi}{2}\lambda_r(r_m{}^2 - r^2))dr \tag{20}$$

$$= 1-\lambda_I\beta^{\frac{2}{\alpha}}\frac{C_\alpha}{K_\alpha}\left(\frac{r_m^2 - \frac{2}{\psi\lambda_r}(1-\exp(-\frac{\psi}{2}\lambda_r r_m{}^2))}{1-\exp(-\frac{\psi}{2}\lambda_r r_m{}^2)}\right)$$

The PDF of the single-hop transmission distance R for the randomly selected neighbor hopping strategy is given by[23]

$$f_R^r(r) = \frac{2r}{r_m{}^2} \qquad 0 < r < r_m \tag{21}$$

Putting together (3) and (21), the per-hop success probability of a packet transmission across the randomly selected neighbor is

$$p_{s,r} \approx 1-\int_0^{r_m} \frac{2r}{r_m^2}\lambda_I\beta^{\frac{2}{\alpha}}\frac{C_\alpha}{K_\alpha} r^2 dr$$

$$= 1-\frac{\lambda_I\beta^{\frac{2}{\alpha}}C_\alpha r_m^2}{2K_\alpha} \tag{22}$$

3.2 Spatial Capacity Density Analysis With Different Hopping Strategies

Theorem 3: In an infinite network following a homogeneous 2-D PPP, the expected single-hop transmission distance for the closest neighbor, furthest neighbor and randomly selected neighbor hopping strategies are given by

$$E_c(R) = \frac{1}{\sqrt{\frac{2\psi}{\pi}\lambda_r}} \times \frac{\sqrt{\frac{2\psi}{\pi}\lambda_r}\, r_m - \exp(\frac{\psi}{2}\lambda_r r_m{}^2)\, erf\left(\sqrt{\frac{\psi}{2}\lambda_r}\, r_m\right)}{1-\exp(\frac{\psi}{2}\lambda_r r_m{}^2)} \tag{23}$$

$$E_f(R) = \frac{1}{\sqrt{\frac{2\psi}{\pi}\lambda_r}} \times \frac{\sqrt{\frac{2\psi}{\pi}\lambda_r}\, r_m - \exp(-\frac{\psi}{2}\lambda_r r_m{}^2)\, erfi\left(\sqrt{\frac{\psi}{2}\lambda_r}\, r_m\right)}{1-\exp(-\frac{\psi}{2}\lambda_r r_m{}^2)} \tag{24}$$

$$E_c(R) = \frac{2}{3} r_m \tag{25}$$

where $erf(\cdot)$ and $erfi(\cdot)$ are the standard and imaginary error functions, respectively, and $erfi(x) = -ierf(ix)$.

Proof: The expected single-hop transmission distance in expressions (23)-(25) can be obtained by evaluating the mean value of R for the PDF of the distance $R \in (0, r_m)$ for each hopping strategy.

Theorem 4: For the closest neighbor, furthest neighbor and randomly selected neighbor hopping strategies, the per-flow throughput T, are respectively given by

$$T_c \approx \frac{q\lambda_I \beta^{\frac{2}{\alpha}} C_\alpha}{4K_\alpha}\left(\frac{K_\alpha}{\lambda_I \beta^{\frac{2}{\alpha}} C_\alpha} - \frac{r_m^2 + \frac{2}{\psi\lambda_r}(1-\exp(\frac{\psi}{2}\lambda_r r_m^2))}{1-\exp(\frac{\psi}{2}\lambda_r r_m^2)}\right) \tag{26}$$

$$T_f \approx \frac{q\lambda_I \beta^{\frac{2}{\alpha}} C_\alpha}{4K_\alpha}\left(\frac{K_\alpha}{\lambda_I \beta^{\frac{2}{\alpha}} C_\alpha} - \frac{r_m^2 - \frac{2}{\psi\lambda_r}(1-\exp(-\frac{\psi}{2}\lambda_r r_m^2))}{1-\exp(-\frac{\psi}{2}\lambda_r r_m^2)}\right) \tag{27}$$

$$T_r \approx \frac{2qK_\alpha - q\lambda_I \beta^{\frac{2}{\alpha}} C_\alpha r_m^2}{8K_\alpha} \tag{28}$$

Proof: As the MAC protocol assumed for each flow is slotted ALOHA, the TASEP model of parallel type can be used for our analysis [24]. Suppose that the reliability of each single hop link is equal to the probability of the successful transmission p_s, then the effective hopping probability in the corresponding parallel TASEP model would be qp_s. We take note that the retransmission scheme can guarantee 100% reliability of the network. Also in [19], given the number of relays $N >> 1$, and the SIR threshold $\beta >> 1$, the throughput of each flow T can be written as

$$T \approx \frac{qp_s}{4} \tag{29}$$

Therefore, by incorporating (14)-(16) into (29), this theorem can be proved.

Moreover, under the aforementioned two assumptions, each node in a typical flow at steady state is independently occupied with probability 1/2, thus the density of interfers in any time slot is:

$$\lambda_I = \frac{\lambda_s Nq}{2} \tag{30}$$

Theorem 5: For the closest neighbor, furthest neighbor and randomly selected neighbor hopping strategies, the expected total progresses of the packet over N+1 hops are given by

$$D_c = \frac{2(N+1)\sin(\frac{\psi}{2})}{\psi\sqrt{\frac{\psi}{2}\lambda_r}} \times \frac{\sqrt{\frac{\psi}{2}\lambda_r} r_m - \exp(\frac{\psi}{2}\lambda_r r_m^2) erf(\sqrt{\frac{\psi}{2}\lambda_r} r_m)}{1-\exp(-\frac{\psi}{2}\lambda_r r_m^2)} \tag{31}$$

$$D_f = \frac{2(N+1)\sin(\frac{\psi}{2})}{\psi\sqrt{\frac{\psi}{2}\lambda_r}} \times \frac{\sqrt{\frac{\psi}{2}\lambda_r} r_m - \exp(-\frac{\psi}{2}\lambda_r r_m^2) erfi(\sqrt{\frac{\psi}{2}\lambda_r} r_m)}{1-\exp(-\frac{\psi}{2}\lambda_r r_m^2)} \tag{32}$$

$$D_r = \frac{4}{3\psi}(N+1)r_m \sin\frac{\psi}{2} \tag{33}$$

Proof: Recalling the definition of the expected total progress D, it can be written as

$$D = (N+1)E[R\cos(\Phi)] = (N+1)E[R]E[\cos(\Phi)] \tag{34}$$

where R is the angle with which each packet traversed at every hop to the destination (see **Fig. 1**) and Φ is uniformly distributed on $(-\psi/2, \psi/2)$, we can obtain the following equation:

$$E[\cos(\Phi)] = \int_{-\frac{\psi}{2}}^{\frac{\psi}{2}} \frac{1}{\psi}\cos(\Phi)d\Phi = \frac{2}{\psi}\sin(\frac{\psi}{2}) \tag{35}$$

This theorem can be proved by combining (23), (24), (25) each with (35) and incorporating into (34) respectively.

Theorem 6: For the closest neighbor, furthest neighbor and randomly selected neighbor hopping strategies, the spatial capacity densities are given by

$$C_{tran\_c} \approx \frac{q\lambda_I\lambda_s\beta^{\frac{2}{\alpha}}C_\alpha(N+1)\sin(\frac{\psi}{2})}{2K_\alpha\psi\sqrt{\frac{\psi}{2}\lambda_r}} \times \frac{\sqrt{\frac{\psi}{2}\lambda_r}r_m - \exp(\frac{\psi}{2}\lambda_r r_m^{\,2})erf(\sqrt{\frac{\psi}{2}\lambda_r}r_m)}{1-\exp(-\frac{\psi}{2}\lambda_r r_m^{\,2})} \times (\frac{K_\alpha}{\lambda_I\beta^{\frac{2}{\alpha}}C_\alpha} - \frac{r_m^2 + \frac{2}{\psi\lambda_r}(1-\exp(\frac{\psi}{2}\lambda_r r_m^2))}{1-\exp(\frac{\psi}{2}\lambda_r r_m^2)}) \quad (36)$$

$$C_{tran\_f} \approx \frac{q\lambda_I\lambda_s\beta^{\frac{2}{\alpha}}C_\alpha(N+1)\sin(\frac{\psi}{2})}{2K_\alpha\psi\sqrt{\frac{\psi}{2}\lambda_r}} \times \frac{\sqrt{\frac{\psi}{2}\lambda_r}r_m - \exp(-\frac{\psi}{2}\lambda_r r_m^{\,2})erfi(\sqrt{\frac{\psi}{2}\lambda_r}r_m)}{1-\exp(-\frac{\psi}{2}\lambda_r r_m^{\,2})} \times (\frac{K_\alpha}{\lambda_I\beta^{\frac{2}{\alpha}}C_\alpha} - \frac{r_m^2 - \frac{2}{\psi\lambda_r}(1-\exp(-\frac{\psi}{2}\lambda_r r_m^2))}{1-\exp(-\frac{\psi}{2}\lambda_r r_m^2)}) \quad (37)$$

$$C_{tran\_r} \approx \frac{(N+1)(2qK_\alpha - q\lambda_I\beta^{\frac{2}{\alpha}}C_\alpha r_m^2)r_m\lambda_s\sin(\frac{\psi}{2})}{6K_\alpha\psi} \quad (38)$$

Proof: Substituting T in (26)-(28) and D in (31)-(33) using the definition of C_{tran} in Sec.2.3, we can obtain the spatial capacity densities for three different hopping strategies.

3.3 Average End-To-End Delay Analysis With Different Hopping Strategies

Theorem 7: For the closest neighbor, furthest neighbor and randomly selected neighbor hopping strategies, the average end-to-end delays for an ALOHA-based flow along N relays are

$$D_{e2e,c} \approx \frac{2(N+1)K_\alpha(1-\exp(\frac{\psi}{2}\lambda_r r_m^2))}{qK_\alpha(1-\exp(\frac{\psi}{2}\lambda_r r_m^2)) - q\beta^{\frac{2}{\alpha}}C_\alpha\lambda_I(r_m^2 + \frac{2}{\psi\lambda_r}(1-\exp(\frac{\psi}{2}\lambda_r r_m^2)))} \quad (39)$$

$$D_{e2e,f} \approx \frac{2(N+1)K_\alpha(1-\exp(-\frac{\psi}{2}\lambda_r r_m^2))}{qK_\alpha(1-\exp(-\frac{\psi}{2}\lambda_r r_m^2)) - q\beta^{\frac{2}{\alpha}}C_\alpha\lambda_I(r_m^2 - \frac{2}{\psi\lambda_r}(1-\exp(-\frac{\psi}{2}\lambda_r r_m^2)))} \quad (40)$$

$$D_{e2e,r} \approx \frac{4K_\alpha(N+2)}{2qK_\alpha - q\lambda_I\beta^{\frac{2}{\alpha}}C_\alpha r_m^4} \quad (41)$$

Proof: We are interested in the performance of the ad hoc network at its steady states (as $t \to \infty$).Since the source nodes are assumed to be always backlogged, this study consider the in-network delay only. As proven in [16], the slotted ALOHA-based flow reaches a steady state and becomes independent of time. The simplified notion $\tau_i := \lim_{t\to\infty}\tau_i[t]$ is to denote the steady state occupancy of node i. As $\tau_i \in \{0,1\}$, we have $P(\tau_i = 1) = E\tau_i$ and $P(\tau_i = 0) = 1 - E\tau_i$. As the particle-hole is symmetry, the average number of packet in the flow at a steady state is $\sum_{i=0}^{N} E\tau_i = 1 + \frac{N}{2}$. Based on the little theorem [25], the average end-to-end delay is:

$$D_{e2e} = \frac{\sum_{i=0}^{N} E\tau_i}{T} = \frac{2+N}{2T} \quad (42)$$

Thus, (39)-(41) can be obtained by inserting the expression of T in (26)-(28) into (42).

4. Numerical Results and Discussions

In this section, we present some numerical results and discussions based on the preceding sections. Unless otherwise stated, we set the values of the network parameter as in **Table 1**.

Table 1. Network, traffic and mobility parameter values

Symbol	Description	Value
q	Access probability	0.2
β	SIR threshold	10dB
r_m	Maximum transmission distance	10m
α	Path-loss exponent	4
λ_0	Node density	0.005
L	Number of antenna branches	3
N	Number of relays	10

We first investigate the effect of the node density λ_0 on the behavior of a multi-hop multi-antenna network with different hopping strategies and scenarios. **Fig.3** illustrates the per-hop success probability versus λ_0. As is shown, when the node density λ_0 rises, the per-hop success probability in each of the three hopping strategies will decrease. The per-hop success probability declines most slowly in the closest neighbor hopping strategy and most sharply in the furthest neighbor hopping strategy. This is because rising λ_0 means increasing number of interfering nodes per unit area, thus the level of the cumulative interference at the intended RX will also go up. In the closest neighbor hopping strategy, when λ_0 increases, there will be more potential RXs within the selection region of the typical TX and the single-hop transmission distance is more likely to be shorter. As a result, the average received signal power will increase with λ_0. Similarly, when the furthest neighbor hopping strategy is used, the average received signal power will degrade with λ_0. Because the distribution of the single-hop transmission distance is not related to λ_0, the average received signal power will remain constant when the randomly selected neighbor hopping strategy is adopted.

Fig.4 shows the spatial capacity density versus node density λ_0. When λ_0 is small, the interference level in the network is low, and the spatial capacity density is not limited by the interference, being an increasing function of the λ_0. It can be observed from **Fig.3** that the per-hop probabilities under different hopping strategies are almost the same with a small λ_0. But since the expected total progress of packet with the furthest neighbor hopping strategy is the largest, it leads that the highest spatial capacity density C_{tran} with the furthest neighbor hopping strategy. When λ_0 increases, outage events are more frequent, and the speed of decrement of per-hop success probability under the furthest neighbor hopping strategy is the highest as shown in **Fig.3**. Since the spatial capacity density is determined by the density of source nodes, the single-hop transmission distance and the per-hop success probability, when λ_0 is large, the closest neighbor is the best hopping strategy. It could be deduced that when the per-hop link is more vulnerable to interference, the single-hop transmission distance should be made as short as possible in order to control interference.

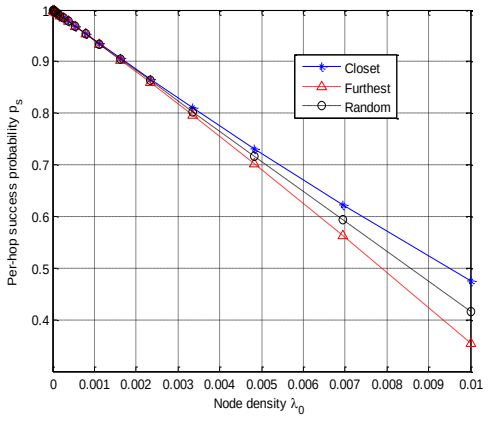

Fig. 3. Per-hop success probability vs. node density

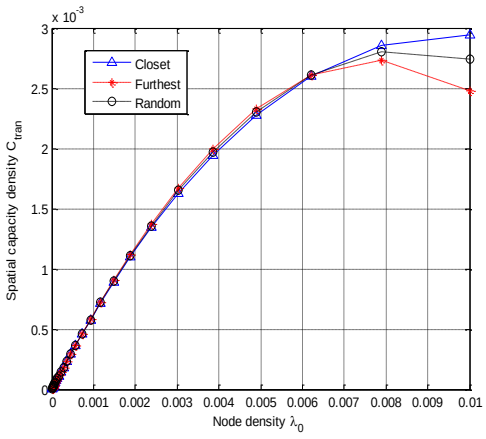

Fig. 4. Spatial capacity density vs. node density

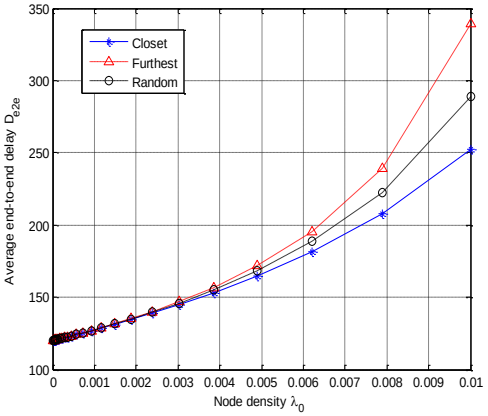

Fig. 5. Average end-to-end delay vs. node density

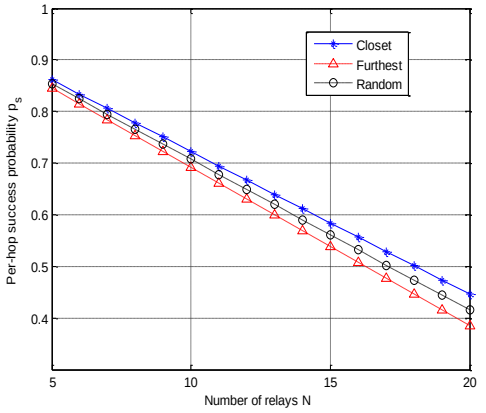

Fig. 6. Per-hop success probability vs. number of relays

Fig.5 demonstrates the average end-to-end delay of networks versus the node density λ_0. From **Fig. 5** we can see that the average end-to-end delay increases most slowly for the closest neighbor hopping strategy with the node density λ_0, and the speed of increment of the randomly selected neighbor hopping strategy lies between that of the furthest neighbor and the closest neighbor. As the previous analysis, the average end-to-end delay in network is in inverse proportion to the per-node success probability, thus the curves in **Fig.5** can be easily understood.

Based on **Fig. 3**, **Fig. 4**, **Fig 5**, the following conclusions can be drawn from a network design stand-point. When the node density λ_0 is low, the differences among the per-hop success probabilities and the end-to-end delays with these three hopping strategies are negligible. With longest single-hop transmission distance, the furtheset neighbor hopping strategy is the best choice. And when the node density λ_0 is high, the closest neighbor hopping strategy has the best performance regarding the metrics of the spatial capacity density and the average end-to-end delay.

Next, we investigate the effect of the number of relays N on the behavior of a network with different hopping strategies and scenarios. As shown in **Fig. 6**, with three hopping strategies, the per-node success probabilities drop as N grows, since the equivalent interfering node density is proportional to N (see(30)). When N becomes larger, the equivalent

interfering node density will increase, the level of cumulative interference will also goes up as a result. Furthermore, with the closest neighbor hopping strategy, the single-hop transmission distance will be the shortest, thus the received signal is thestrongest, therefore, the per-hop success probability decreases most slowly in the closest neighbor hopping strategy with N and the speed of decrement of the randomly selected neighbor hopping strategy lies between that of the furthest neighbor and the closest neighbor with a similar reason.

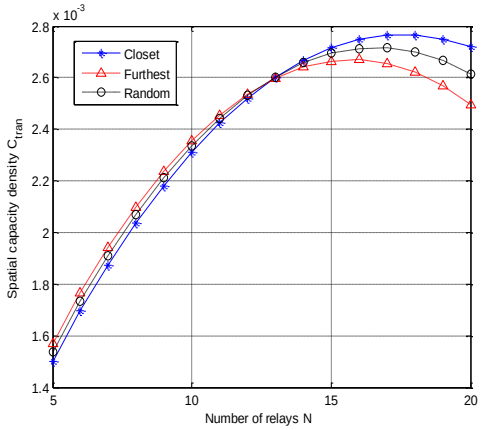

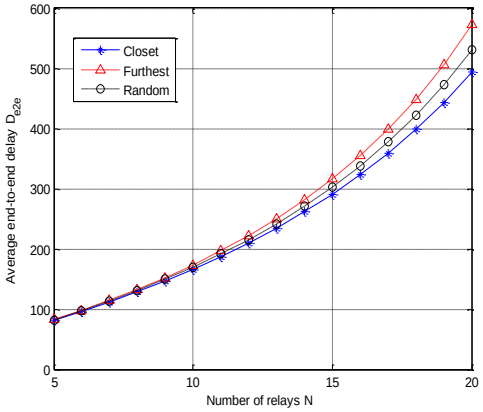

Fig. 7. Spatial capacity density vs. number of relays **Fig. 8.** Average end-to-end delay vs. number of relays

Fig.7 illustrates the spatial capacity density versus the number of relays N. As shown in this figure, when N is small, increasing N means increasing the expected total progress. The spatial capacity density is an increasing function of N. As the expected single-hop distance with the furthest neighbor hopping strategy is the longest, the furthest neighbor hopping strategy is the best choice. But when N is taken a large value, the equivalent interfering node density is an important determinantfor the spatial capacity density. Therefore when N increases, the spatial capacity density will reduce. As the per-hop success probability decreases most slowly with N for the closest neighbor hopping strategy, it is the best hopping strategy is to choose.

As shown in **Fig. 8**, the average end-to-end delay increases most slowly for the closest neighbor hopping strategy with the number of relays N, and the speed of increment of the randomly selected neighbor hopping strategy lies between that of the furthest neighbor and the closest neighbor. The explanation of this figure is similar as **Fig. 5**.

Through **Fig. 6**, **Fig .7**, **Fig. 8**, it can be concluded that when N is small, choosing the furthest neighbor hopping strategy is most appropriate since the spatial capacity density is the largest of that hopping strategy and differences among the average end-to-end delays of the three RX selection strategies can be neglected. When N is large, the best hopping strategy is the closest neighbor hopping strategy regarding both the spatial capacity density and the end-to-end delay performance metrics.

Then we investigate the effect of the number of antennas L on the behavior of a network with different hopping strategies and scenarios. As shown in **Fig. 9**, when L increases, per-hop success probabilities will rise. This is because diversity techniques can mitigate the effects of multi-path fading. And the detailed reason why the per-hop success probability with the closest neighbor strategy is the largest is similar to our previous analysis.

Fig. 10 and **Fig. 11** illustrate the spatial capacity density and the end-to-end delay performance versus the number of antennas L respectively. **Fig. 10** indicates when L=1 or without spatial diversity, the spatial capacity density with the closest neighbor hopping is the largest and when L is greater than 1, that with the furthest neighbor hopping strategy is the largest. This is because the difference of the per-hop success probability between the closest and furthest neighbor hopping strategies is very large when L=1 (see **Fig. 9**), although the expected single-hop distance with the furthest neighbor hopping is the largest, it cannot significantly improve the performance of the spatial capacity density compared to the closest neighbor hopping strategy. However, as L increases, the gap of per-hop success probability between these two hopping strategies will fall proportionally, thus the furthest neighbor hopping strategy will be preferrable. **Fig. 11** shows the average end-to-end delay decreases as L grows.

So, it could be observed from, **Fig.9**, **Fig. 10**, **Fig. 11** that when L=1, the closest neighbor hopping strategy since is the best, with the largest spatial capacity density and the lowest end-to-end delay. And when $L>1$, the best hopping strategy is the futhest neighbor hopping strategy regarding these two performance metrics.

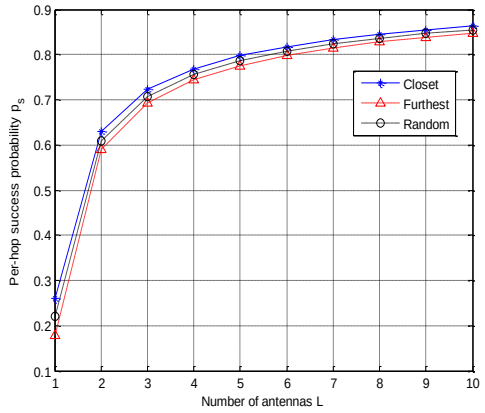

Fig. 9. Per-hop success probability vs. number of

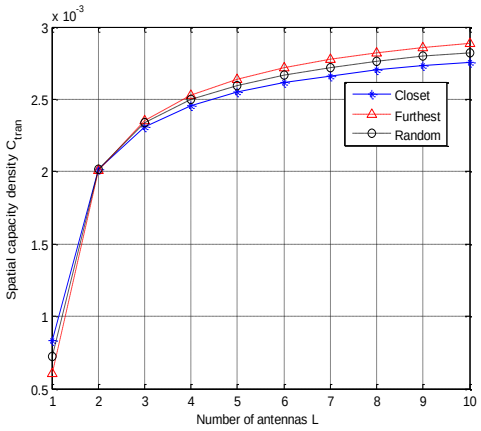

Fig. 10. Spatial capacity density vs. number of antennas

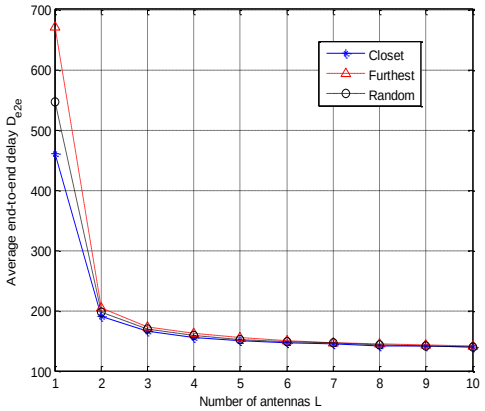

Fig. 11. Average end-to-end delay vs. number

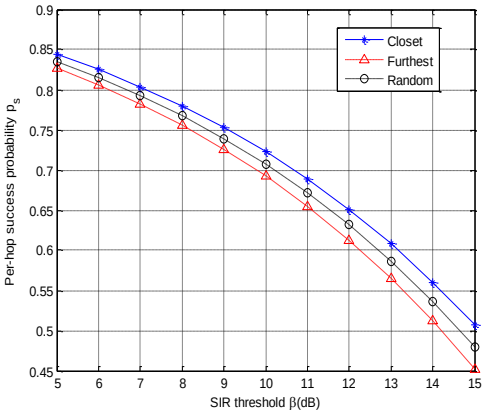

Fig. 12. Per-hop success probability vs. SIR antennas

Finally, the effect of SIR threshold β is taken into account on behavior of a network with different hopping strategies and scenarios. The performance metrics of per-hop success probability, spatial capacity density and average end-to-end delay are plotted against the SIR threshold β in **Fig. 12**, **Fig. 13**, **Fig. 14**, respectively. As shown in **Fig. 12**, as β becomes larger, the outage probability will increase, and the per-hop success probability will deduce, and accordingly, the average end-to-end delay will increase as shown in **Fig. 14**. Furthermore, from **Fig. 13**, when β is small, the spatial capacity density with the furthest neighbor hopping strategy is the largest, but as β grows, the closest neighbor hopping strategy is abetter choice with regard to that metric. So by integrating the observations from **Fig. 12**, **Fig. 13**, **Fig. 14**, we can conclude that when β is small, the furthest neighbor hopping strategy is the best choice, and when β is large, the closest neighbor hopping strategy is the best choice.

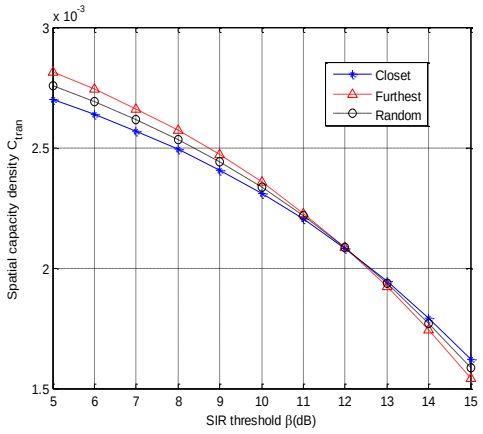

Fig. 13. Spatial capacity density vs. SIR threshold

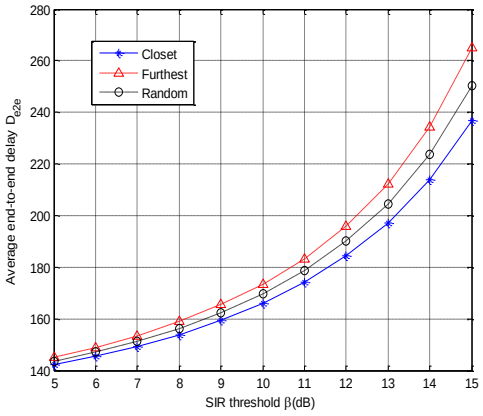

Fig. 14. Average end-to-end delay vs. SIR threshold

5. Conclusion

In this paper, we have studied the performance of multi-hop multi-antenna wireless network operating under three hopping strategies - closest neighbor, furthest neighbor and randomly selected neighbor hopping strategies. Using concepts and tools from the stochastic geometry and TASEP model, closed-form expressions of two main end-to-end performance metrics, the spatial capacity density and the average end-to-end delay, are derived. Based on these metrics, some insights on choosing the best hopping strategy can be provided which are valuable to network design. This formulation allows us to identify the network operating conditions under which a given hopping strategy outperforms the others. In the future we plan to study issues regarding some other MAC protocols as well as the more practical routing strategies in multi-hop wireless networks.

References

[1] P. Gupta and P. R. Kumar, "The capacity of wireless networks," *IEEE Transactions on Information Theory,* vol. 46, pp. 388-404, Mar. 2000.Article (CrossRef Link)

[2] F. Xue*, et al.*, "The transport capacity of wireless networks over fading channels," *IEEE*

Transactions on Information Theory, vol. 51, pp. 834-847, Mar 2005. Article(CrossRef Link)

[3] L. L. Xie and P. R. Kumar, "A network information theory for wireless communication: Scaling laws and optimal operation," *IEEE Transactions on Information Theory,* vol. 50, pp. 748-767, May 2004. Article(CrossRef Link)

[4] S. P. Weber, *et al.*, "Transmission capacity of wireless ad hoc networks with outage constraints," *IEEE Transactions on Information Theory,* vol. 51, pp. 4091-4102, 2005. Article(CrossRef Link)

[5] D. Stoyan, *et al.*, *Stochastic geometry and its applications* vol. 2: Wiley New York, 1996. Article(CrossRef Link)

[6] A. Baddeley, "Spatial point processes and their applications," *Stochastic Geometry,* vol. 1892, pp. 1-75, 2007. Article(CrossRef Link)

[7] S. Weber, *et al.*, "An Overview of the Transmission Capacity of Wireless Networks," *IEEE Transactions on Communications,* vol. 58, pp. 3593-3604, Dec 2010. Article(CrossRef Link)

[8] 13N. Jindal, S. Weber, and J.G.Andrews."Fractional power control for decentralized wireless networks".*IEEE Transactions on Wireless Communication*, vol.7,no.12,pp. 5482-5492,Jun 2008. Article(CrossRef Link)

[9] S.Weber, J.G.Andrews, et al."Transmission capacity of wireless ad hoc networks with successive interference cancellation".*IEEE Transactions on Information Theory*, vol.53,no.8, pp.2799-2814, Aug.2007. Article(CrossRef Link)

[10] S.Weber, J.G. Andrews, and N. Jindal."The effect of fading, channel inversion, and threshold scheduling on ad hoc networks,"*IEEE Transactions on Information Theory*, vol.53. 53(11): pp.4127-4149,Nov.2007. Article(CrossRef Link)

[11] J. G. Andrews, *et al.*, "Random Access Transport Capacity," *IEEE Transactions on Wireless Communications,* vol. 9, pp. 2101-2111, Jun 2010. Article(CrossRef Link)

[12] R. Vaze, "Throughput-Delay-Reliability Tradeoff with ARQ in Wireless Ad Hoc Networks," *IEEE Transactions on Wireless Communications,* vol. 10, pp. 2142-2149, Jul 2011. Article(CrossRef Link)

[13] P. H. J. Nardelli, *et al.*, "Multi-Hop Aggregate Information Efficiency in Wireless Ad Hoc Networks," in *ICC 2009 International Conference on Communications*, 2009, pp. 1-6. Article(CrossRef Link)

[14] P. H. J. Nardelli, *et al.*, "Efficiency of Wireless Networks under Different Hopping Strategies," *IEEE Transactions on Wireless Communications,* vol. 11, pp. 15-20, 2012. Article(CrossRef Link)

[15] S. Srinivasa and M. Haenggi, "The TASEP: A Statistical Mechanics Tool to Study the Performance of Wireless Line Networks," in *Proc. of 19th International Conference on Computer Communications and Networks* 2010, pp. 1-6. Article(CrossRef Link)

[16] N. Rajewsky, *et al.*, "The asymmetric exclusion process: Comparison of update procedures," *Journal of Statistical Physics,* vol. 92, pp. 151-194, Jul 1998. Article(CrossRef Link)

[17] L. Di, *et al.*, "A selection region based routing protocol for random mobile ad hoc networks," in *IEEE GLOBECOM 2010* 2010, pp. 104-108. Article(CrossRef Link)

[18] P. H. J. Nardelli and G. T. F. de Abreu, "On Hopping Strategies for Autonomous Wireless Networks," in *IEEE GLOBECOM 2009.*, 2009, pp. 1-6. Article(CrossRef Link)

[19] S. Srinivasa and M. Haenggi, "Combining stochastic geometry and statistical mechanics for the analysis and design of ad hoc networks," *in preparation for submission to Elsevier Ad Hoc Networks.* Article(CrossRef Link).

[20] A. Shah and A. M. Haimovich, "Performance analysis of maximal ratio combining and comparison with optimum combining for mobile radio communications with cochannel interference," *IEEE Transactions on Vehicular Technology,* vol. 49, pp. 1454-1463, 2000. Article(CrossRef Link)

[21] A. M. Hunter, *et al.*, "Transmission capacity of ad hoc networks with spatial diversity," *IEEE Transactions on Wireless Communications,* vol. 7, pp. 5058-5071, 2008. Article(CrossRef Link)

[22] J. F. C. Kingman, *Poisson processes*: Wiley Online Library, 1993. Article(CrossRef Link)

[23] C. H. Chen, *et al.*, "Expected Density of Progress for Wireless Ad Hoc Networks with Nakagami-m Fading," *IEEE 2011 ICC,* 2011. Article (CrossRef Link)

[24] M. R. Evans, *et al.*, "Exact solution of a cellular automaton for traffic," *Journal of Statistical Physics,* vol. 95, pp. 45-96, Apr. 1999. Article(CrossRef Link)

[25] L. Kleinrock, "Queueing Systems. Volume 1: Theory," 1975. Article(CrossRef Link)

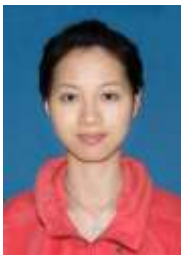

Hu Han received the M.S.degree in Telecommunication and Information Engineering from Nanjing University of Posts and Telecommunications (NUPT), Jiangsu, China in April 2010. Now she is a Ph.D.candidate in Telecommunication and Information Engineering at NUPT.Her main research interests includes stochastic geometry and performance evaluation of wireless networks.

Hongbo Zhu is currently a Professor in Jiangsu Key Laboratory of Wireless Communications, NUPT. He is the Vice Chairman of SG3 of ITU Radio Communication Bureau (ITU-R). He has authored and co-authored over 200 technical papers published in various journals and conferences. His research interests include wireless communication theory and radio propagation in wireless communications.

Qi Zhu received the M.S. degree in radio engineering from Nanjing University of Posts and Telecommunications in 1989. Now she is a professor in the Department of Telecommunication and Information Engineering, NUPT, Jiangsu, China. Her research interests include radio resource management, heterogeneous networks, and performance evaluation of wireless networks.